

Observation of the Production of a W Boson in Association with a Single Charm Quark

T. Aaltonen,²¹ B. Álvarez González^{z,9} S. Amerio,⁴⁰ D. Amidei,³² A. Anastassov^{x,15} A. Annovi,¹⁷ J. Antos,¹² G. Apollinari,¹⁵ J.A. Appel,¹⁵ T. Arisawa,⁵⁴ A. Artikov,¹³ J. Asaadi,⁴⁹ W. Ashmanskas,¹⁵ B. Auerbach,⁵⁷ A. Aurisano,⁴⁹ F. Azfar,³⁹ W. Badgett,¹⁵ T. Bae,²⁵ A. Barbaro-Galtieri,²⁶ V.E. Barnes,⁴⁴ B.A. Barnett,²³ P. Barria^{hh,42} P. Bartos,¹² M. Bauce^{ff,40} F. Bedeschi,⁴² S. Behari,²³ G. Bellettini^{gg,42} J. Bellinger,⁵⁶ D. Benjamin,¹⁴ A. Beretvas,¹⁵ A. Bhatti,⁴⁶ D. Bisello^{ff,40} I. Bizjak,²⁸ K.R. Bland,⁵ B. Blumenfeld,²³ A. Bocci,¹⁴ A. Bodek,⁴⁵ D. Bortoletto,⁴⁴ J. Boudreau,⁴³ A. Boveia,¹¹ L. Brigliadori^{ee,6} C. Bromberg,³³ E. Brucken,²¹ J. Budagov,¹³ H.S. Budd,⁴⁵ K. Burkett,¹⁵ G. Busetto^{ff,40} P. Bussey,¹⁹ A. Buzatu,³¹ A. Calamba,¹⁰ C. Calancha,²⁹ S. Camarda,⁴ M. Campanelli,²⁸ M. Campbell,³² F. Canelli,^{11,15} B. Carls,²² D. Carlsmith,⁵⁶ R. Carosi,⁴² S. Carrillo^{m,16} S. Carron,¹⁵ B. Casal^{k,9} M. Casarsa,⁵⁰ A. Castro^{ee,6} P. Catastini,²⁰ D. Cauz,⁵⁰ V. Cavaliere,²² M. Cavalli-Sforza,⁴ A. Cerri^{f,26} L. Cerrito^{s,28} Y.C. Chen,¹ M. Chertok,⁷ G. Chiarelli,⁴² G. Chlachidze,¹⁵ F. Chlebana,¹⁵ K. Cho,²⁵ D. Chokheli,¹³ W.H. Chung,⁵⁶ Y.S. Chung,⁴⁵ M.A. Ciocci^{hh,42} A. Clark,¹⁸ C. Clarke,⁵⁵ G. Compostella^{ff,40} M.E. Convery,¹⁵ J. Conway,⁷ M. Corbo,¹⁵ M. Cordelli,¹⁷ C.A. Cox,⁷ D.J. Cox,⁷ F. Crescioli^{gg,42} J. Cuevas^{z,9} R. Culbertson,¹⁵ D. Dagenhart,¹⁵ N. d'Ascenzo^{w,15} M. Datta,¹⁵ P. de Barbaro,⁴⁵ M. Dell'Orso^{gg,42} L. Demortier,⁴⁶ M. Deninno,⁶ F. Devoto,²¹ M. d'Errico^{ff,40} A. Di Canto^{gg,42} B. Di Ruzza,¹⁵ J.R. Dittmann,⁵ M. D'Onofrio,²⁷ S. Donati^{gg,42} P. Dong,¹⁵ M. Dorigo,⁵⁰ T. Dorigo,⁴⁰ K. Ebina,⁵⁴ A. Elagin,⁴⁹ A. Eppig,³² R. Erbacher,⁷ S. Errede,²² N. Ershaidat^{dd,15} R. Eusebi,⁴⁹ S. Farrington,³⁹ M. Feindt,²⁴ J.P. Fernandez,²⁹ R. Field,¹⁶ G. Flanagan^{u,15} R. Forrest,⁷ M.J. Frank,⁵ M. Franklin,²⁰ J.C. Freeman,¹⁵ Y. Funakoshi,⁵⁴ I. Furic,¹⁶ M. Gallinaro,⁴⁶ J.E. Garcia,¹⁸ A.F. Garfinkel,⁴⁴ P. Garosi^{hh,42} H. Gerberich,²² E. Gerchtein,¹⁵ S. Giagu,⁴⁷ V. Giakoumopoulou,³ P. Giannetti,⁴² K. Gibson,⁴³ C.M. Ginsburg,¹⁵ N. Giokaris,³ P. Giromini,¹⁷ G. Giurgiu,²³ V. Glagolev,¹³ D. Glenzinski,¹⁵ M. Gold,³⁵ D. Goldin,⁴⁹ N. Goldschmidt,¹⁶ A. Golossanov,¹⁵ G. Gomez,⁹ G. Gomez-Ceballos,³⁰ M. Goncharov,³⁰ O. González,²⁹ I. Gorelov,³⁵ A.T. Goshaw,¹⁴ K. Goulianos,⁴⁶ S. Grinstein,⁴ C. Grosso-Pilcher,¹¹ R.C. Group^{53,15} J. Guimaraes da Costa,²⁰ S.R. Hahn,¹⁵ E. Halkiadakis,⁴⁸ A. Hamaguchi,³⁸ J.Y. Han,⁴⁵ F. Happacher,¹⁷ K. Hara,⁵¹ D. Hare,⁴⁸ M. Hare,⁵² R.F. Harr,⁵⁵ K. Hatakeyama,⁵ C. Hays,³⁹ M. Heck,²⁴ J. Heinrich,⁴¹ M. Herndon,⁵⁶ S. Hewamanage,⁵ A. Hocker,¹⁵ W. Hopkins^{g,15} D. Horn,²⁴ S. Hou,¹ R.E. Hughes,³⁶ M. Hurwitz,¹¹ U. Husemann,⁵⁷ N. Hussain,³¹ M. Hussein,³³ J. Huston,³³ G. Introzzi,⁴² M. Iori^{jj,47} A. Ivanov^{p,7} E. James,¹⁵ D. Jang,¹⁰ B. Jayatilaka,¹⁴ E.J. Jeon,²⁵ S. Jindariani,¹⁵ M. Jones,⁴⁴ K.K. Joo,²⁵ S.Y. Jun,¹⁰ T.R. Junk,¹⁵ T. Kamon^{25,49} P.E. Karchin,⁵⁵ A. Kashi,⁵ Y. Kato^{o,38} W. Ketchum,¹¹ J. Keung,⁴¹ V. Khotilovich,⁴⁹ B. Kilminster,¹⁵ D.H. Kim,²⁵ H.S. Kim,²⁵ J.E. Kim,²⁵ M.J. Kim,¹⁷ S.B. Kim,²⁵ S.H. Kim,⁵¹ Y.K. Kim,¹¹ Y.J. Kim,²⁵ N. Kimura,⁵⁴ M. Kirby,¹⁵ S. Klimenko,¹⁶ K. Knoepfel,¹⁵ K. Kondo^{*,54} D.J. Kong,²⁵ J. Konigsberg,¹⁶ A.V. Kotwal,¹⁴ M. Kreps,²⁴ J. Kroll,⁴¹ D. Krop,¹¹ M. Kruse,¹⁴ V. Krutelyov^{c,49} T. Kuhr,²⁴ M. Kurata,⁵¹ S. Kwang,¹¹ A.T. Laasanen,⁴⁴ S. Lami,⁴² S. Lammel,¹⁵ M. Lancaster,²⁸ R.L. Lander,⁷ K. Lannon^{y,36} A. Lath,⁴⁸ G. Latino^{hh,42} T. LeCompte,² E. Lee,⁴⁹ H.S. Lee^{q,11} J.S. Lee,²⁵ S.W. Lee^{bb,49} S. Leo^{gg,42} S. Leone,⁴² J.D. Lewis,¹⁵ A. Limosani^{t,14} C.-J. Lin,²⁶ M. Lindgren,¹⁵ E. Lipeles,⁴¹ A. Lister,¹⁸ D.O. Litvintsev,¹⁵ C. Liu,⁴³ H. Liu,⁵³ Q. Liu,⁴⁴ T. Liu,¹⁵ S. Lockwitz,⁵⁷ A. Loginov,⁵⁷ D. Lucchesi^{ff,40} J. Lueck,²⁴ P. Lujan,²⁶ P. Lukens,¹⁵ G. Lungu,⁴⁶ J. Lys,²⁶ R. Lysak^{e,12} R. Madrak,¹⁵ K. Maeshima,¹⁵ P. Maestro^{hh,42} S. Malik,⁴⁶ G. Manca^{a,27} A. Manousakis-Katsikakis,³ F. Margaroli,⁴⁷ C. Marino,²⁴ M. Martínez,⁴ P. Mastrandrea,⁴⁷ K. Matera,²² M.E. Mattson,⁵⁵ A. Mazzacane,¹⁵ P. Mazzanti,⁶ K.S. McFarland,⁴⁵ P. McIntyre,⁴⁹ R. McNulty^{j,27} A. Mehta,²⁷ P. Mehtala,²¹ C. Mesropian,⁴⁶ T. Miao,¹⁵ D. Mietlicki,³² A. Mitra,¹ H. Miyake,⁵¹ S. Moed,¹⁵ N. Moggi,⁶ M.N. Mondragon^{m,15} C.S. Moon,²⁵ R. Moore,¹⁵ M.J. Morello^{ii,42} J. Morlock,²⁴ P. Movilla Fernandez,¹⁵ A. Mukherjee,¹⁵ Th. Muller,²⁴ P. Murat,¹⁵ M. Mussini^{ee,6} J. Nachtman^{n,15} Y. Nagai,⁵¹ J. Naganoma,⁵⁴ I. Nakano,³⁷ A. Napier,⁵² J. Nett,⁴⁹ C. Neu,⁵³ M.S. Neubauer,²² J. Nielsen^{d,26} L. Nodulman,² S.Y. Noh,²⁵ O. Norriella,²² L. Oakes,³⁹ S.H. Oh,¹⁴ Y.D. Oh,²⁵ I. Oksuzian,⁵³ T. Okusawa,³⁸ R. Orava,²¹ L. Ortolan,⁴ S. Pagan Griso^{ff,40} C. Pagliarone,⁵⁰ E. Palencia^{f,9} V. Papadimitriou,¹⁵ A.A. Paramonov,² J. Patrick,¹⁵ G. Pauletta^{kk,50} M. Paulini,¹⁰ C. Paus,³⁰ D.E. Pellett,⁷ A. Penzo,⁵⁰ T.J. Phillips,¹⁴ G. Piacentino,⁴² E. Pianori,⁴¹ J. Pilot,³⁶ K. Pitts,²² C. Plager,⁸ L. Pondrom,⁵⁶ S. Poprocki^{g,15} K. Potamianos,⁴⁴ F. Prokoshin^{cc,13} A. Pranko,²⁶ F. Ptohos^{h,17} G. Punzi^{gg,42} A. Rahaman,⁴³ V. Ramakrishnan,⁵⁶ N. Ranjan,⁴⁴ I. Redondo,²⁹ P. Renton,³⁹ M. Rescigno,⁴⁷ T. Riddick,²⁸ F. Rimondi^{ee,6} L. Ristori^{42,15} A. Robson,¹⁹ T. Rodrigo,⁹ T. Rodriguez,⁴¹ E. Rogers,²² S. Rolli^{i,52} R. Roser,¹⁵ F. Ruffini^{hh,42} A. Ruiz,⁹ J. Russ,¹⁰ V. Rusu,¹⁵ A. Safonov,⁴⁹ W.K. Sakumoto,⁴⁵ Y. Sakurai,⁵⁴ L. Santi^{kk,50} K. Sato,⁵¹

V. Saveliev^{w,15} A. Savoy-Navarro^{aa,15} P. Schlabach,¹⁵ A. Schmidt,²⁴ E.E. Schmidt,¹⁵ T. Schwarz,¹⁵ L. Scodellaro,⁹ A. Scribano^{hh,42} F. Scuri,⁴² S. Seidel,³⁵ Y. Seiya,³⁸ A. Semenov,¹³ F. Sforza^{hh,42} S.Z. Shalhout,⁷ T. Shears,²⁷ P.F. Shepard,⁴³ M. Shimojima^{v,51} M. Shochet,¹¹ I. Shreyber-Tecker,³⁴ A. Simonenko,¹³ P. Sinervo,³¹ K. Sliwa,⁵² J.R. Smith,⁷ F.D. Snider,¹⁵ A. Soha,¹⁵ V. Sorin,⁴ H. Song,⁴³ P. Squillacioti^{hh,42} M. Stancari,¹⁵ R. St. Denis,¹⁹ B. Stelzer,³¹ O. Stelzer-Chilton,³¹ D. Stentz^{x,15} J. Strologas,³⁵ G.L. Strycker,³² Y. Sudo,⁵¹ A. Sukhanov,¹⁵ I. Suslov,¹³ K. Takemasa,⁵¹ Y. Takeuchi,⁵¹ J. Tang,¹¹ M. Tecchio,³² P.K. Teng,¹ J. Thom^{g,15} J. Thome,¹⁰ G.A. Thompson,²² E. Thomson,⁴¹ D. Toback,⁴⁹ S. Tokar,¹² K. Tollefson,³³ T. Tomura,⁵¹ D. Tonelli,¹⁵ S. Torre,¹⁷ D. Torretta,¹⁵ P. Totaro,⁴⁰ M. Trovato^{ii,42} F. Ukegawa,⁵¹ S. Uozumi,²⁵ A. Varganov,³² F. Vázquez^{m,16} G. Velev,¹⁵ C. Vellidis,¹⁵ M. Vidal,⁴⁴ I. Vila,⁹ R. Vilar,⁹ J. Vizán,⁹ M. Vogel,³⁵ G. Volpi,¹⁷ P. Wagner,⁴¹ R.L. Wagner,¹⁵ T. Wakisaka,³⁸ R. Wallny,⁸ S.M. Wang,¹ A. Warburton,³¹ D. Waters,²⁸ W.C. Wester III,¹⁵ D. Whiteson^{b,41} A.B. Wicklund,² E. Wicklund,¹⁵ S. Wilbur,¹¹ F. Wick,²⁴ H.H. Williams,⁴¹ J.S. Wilson,³⁶ P. Wilson,¹⁵ B.L. Winer,³⁶ P. Wittich^{g,15} S. Wolbers,¹⁵ H. Wolfe,³⁶ T. Wright,³² X. Wu,¹⁸ Z. Wu,⁵ K. Yamamoto,³⁸ D. Yamato,³⁸ T. Yang,¹⁵ U.K. Yang^{r,11} Y.C. Yang,²⁵ W.-M. Yao,²⁶ G.P. Yeh,¹⁵ K. Yi^{n,15} J. Yoh,¹⁵ K. Yorita,⁵⁴ T. Yoshida^{l,38} G.B. Yu,¹⁴ I. Yu,²⁵ S.S. Yu,¹⁵ J.C. Yun,¹⁵ A. Zanetti,⁵⁰ Y. Zeng,¹⁴ C. Zhou,¹⁴ and S. Zucchelli^{ee6}

(CDF Collaboration[†])

¹*Institute of Physics, Academia Sinica, Taipei, Taiwan 11529, Republic of China*

²*Argonne National Laboratory, Argonne, Illinois 60439, USA*

³*University of Athens, 157 71 Athens, Greece*

⁴*Institut de Física d'Altes Energies, ICREA, Universitat Autònoma de Barcelona, E-08193, Bellaterra (Barcelona), Spain*

⁵*Baylor University, Waco, Texas 76798, USA*

⁶*Istituto Nazionale di Fisica Nucleare Bologna, ^{ee} University of Bologna, I-40127 Bologna, Italy*

⁷*University of California, Davis, Davis, California 95616, USA*

⁸*University of California, Los Angeles, Los Angeles, California 90024, USA*

⁹*Instituto de Física de Cantabria, CSIC-University of Cantabria, 39005 Santander, Spain*

¹⁰*Carnegie Mellon University, Pittsburgh, Pennsylvania 15213, USA*

¹¹*Enrico Fermi Institute, University of Chicago, Chicago, Illinois 60637, USA*

¹²*Comenius University, 842 48 Bratislava, Slovakia; Institute of Experimental Physics, 040 01 Kosice, Slovakia*

¹³*Joint Institute for Nuclear Research, RU-141980 Dubna, Russia*

¹⁴*Duke University, Durham, North Carolina 27708, USA*

¹⁵*Fermi National Accelerator Laboratory, Batavia, Illinois 60510, USA*

¹⁶*University of Florida, Gainesville, Florida 32611, USA*

¹⁷*Laboratori Nazionali di Frascati, Istituto Nazionale di Fisica Nucleare, I-00044 Frascati, Italy*

¹⁸*University of Geneva, CH-1211 Geneva 4, Switzerland*

¹⁹*Glasgow University, Glasgow G12 8QQ, United Kingdom*

²⁰*Harvard University, Cambridge, Massachusetts 02138, USA*

²¹*Division of High Energy Physics, Department of Physics,*

University of Helsinki and Helsinki Institute of Physics, FIN-00014, Helsinki, Finland

²²*University of Illinois, Urbana, Illinois 61801, USA*

²³*The Johns Hopkins University, Baltimore, Maryland 21218, USA*

²⁴*Institut für Experimentelle Kernphysik, Karlsruhe Institute of Technology, D-76131 Karlsruhe, Germany*

²⁵*Center for High Energy Physics: Kyungpook National University,*

Daegu 702-701, Korea; Seoul National University, Seoul 151-742,

Korea; Sungkyunkwan University, Suwon 440-746,

Korea; Korea Institute of Science and Technology Information,

Daejeon 305-806, Korea; Chonnam National University, Gwangju 500-757,

Korea; Chonbuk National University, Jeonju 561-756, Korea

²⁶*Ernest Orlando Lawrence Berkeley National Laboratory, Berkeley, California 94720, USA*

²⁷*University of Liverpool, Liverpool L69 7ZE, United Kingdom*

²⁸*University College London, London WC1E 6BT, United Kingdom*

²⁹*Centro de Investigaciones Energéticas Medioambientales y Tecnológicas, E-28040 Madrid, Spain*

³⁰*Massachusetts Institute of Technology, Cambridge, Massachusetts 02139, USA*

³¹*Institute of Particle Physics: McGill University, Montréal, Québec,*

Canada H3A 2T8; Simon Fraser University, Burnaby, British Columbia,

Canada V5A 1S6; University of Toronto, Toronto, Ontario,

Canada M5S 1A7; and TRIUMF, Vancouver, British Columbia, Canada V6T 2A3

³²*University of Michigan, Ann Arbor, Michigan 48109, USA*

³³*Michigan State University, East Lansing, Michigan 48824, USA*

³⁴*Institution for Theoretical and Experimental Physics, ITEP, Moscow 117259, Russia*

³⁵*University of New Mexico, Albuquerque, New Mexico 87131, USA*

³⁶*The Ohio State University, Columbus, Ohio 43210, USA*

³⁷Okayama University, Okayama 700-8530, Japan

³⁸Osaka City University, Osaka 588, Japan

³⁹University of Oxford, Oxford OX1 3RH, United Kingdom

⁴⁰Istituto Nazionale di Fisica Nucleare, Sezione di Padova-Trento, ^{ff}University of Padova, I-35131 Padova, Italy

⁴¹University of Pennsylvania, Philadelphia, Pennsylvania 19104, USA

⁴²Istituto Nazionale di Fisica Nucleare Pisa, ^{gg}University of Pisa,

^{hh}University of Siena and ⁱⁱScuola Normale Superiore, I-56127 Pisa, Italy

⁴³University of Pittsburgh, Pittsburgh, Pennsylvania 15260, USA

⁴⁴Purdue University, West Lafayette, Indiana 47907, USA

⁴⁵University of Rochester, Rochester, New York 14627, USA

⁴⁶The Rockefeller University, New York, New York 10065, USA

⁴⁷Istituto Nazionale di Fisica Nucleare, Sezione di Roma 1,

^{jj}Sapienza Università di Roma, I-00185 Roma, Italy

⁴⁸Rutgers University, Piscataway, New Jersey 08855, USA

⁴⁹Texas A&M University, College Station, Texas 77843, USA

⁵⁰Istituto Nazionale di Fisica Nucleare Trieste/Udine,

I-34100 Trieste, ^{kk}University of Udine, I-33100 Udine, Italy

⁵¹University of Tsukuba, Tsukuba, Ibaraki 305, Japan

⁵²Tufts University, Medford, Massachusetts 02155, USA

⁵³University of Virginia, Charlottesville, Virginia 22906, USA

⁵⁴Waseda University, Tokyo 169, Japan

⁵⁵Wayne State University, Detroit, Michigan 48201, USA

⁵⁶University of Wisconsin, Madison, Wisconsin 53706, USA

⁵⁷Yale University, New Haven, Connecticut 06520, USA

(Dated: September 11, 2012)

The first observation of the production of a W boson with a single charm quark (c) jet in $p\bar{p}$ collisions at $\sqrt{s} = 1.96$ TeV is reported. The analysis uses data corresponding to 4.3 fb^{-1} , recorded with the CDF II detector at the Fermilab Tevatron. Charm quark candidates are selected through the identification of an electron or muon from charm-hadron semileptonic decay within a hadronic jet, and a Wc signal is observed with a significance of 5.7 standard deviations. The production cross section $\sigma_{Wc}(p_{Tc} > 20 \text{ GeV}/c, |\eta_c| < 1.5) \times B(W \rightarrow \ell\nu)$ is measured to be $13.6^{+3.4}_{-3.1}$ pb and is in agreement with theoretical expectations. From this result the magnitude of the quark-mixing matrix element V_{cs} is derived, $|V_{cs}| = 1.08 \pm 0.16$ along with a lower limit of $|V_{cs}| > 0.71$ at the 95% confidence level, assuming that the Wc production through c to s quark coupling is dominant.

PACS numbers: 13.38.Be, 13.20.Fc, 13.85.Lg

*Deceased

[†]With visitors from ^aIstituto Nazionale di Fisica Nucleare, Sezione di Cagliari, 09042 Monserrato (Cagliari), Italy, ^bUniversity of CA Irvine, Irvine, CA 92697, USA, ^cUniversity of CA Santa Barbara, Santa Barbara, CA 93106, USA, ^dUniversity of CA Santa Cruz, Santa Cruz, CA 95064, USA, ^eInstitute of Physics, Academy of Sciences of the Czech Republic, Czech Republic, ^fCERN, CH-1211 Geneva, Switzerland, ^gCornell University, Ithaca, NY 14853, USA, ^hUniversity of Cyprus, Nicosia CY-1678, Cyprus, ⁱOffice of Science, U.S. Department of Energy, Washington, DC 20585, USA, ^jUniversity College Dublin, Dublin 4, Ireland, ^kETH, 8092 Zurich, Switzerland, ^lUniversity of Fukui, Fukui City, Fukui Prefecture, Japan 910-0017, ^mUniversidad Iberoamericana, Mexico D.F., Mexico, ⁿUniversity of Iowa, Iowa City, IA 52242, USA, ^oKinki University, Higashi-Osaka City, Japan 577-8502, ^pKansas State University, Manhattan, KS 66506, USA, ^qKorea University, Seoul, 136-713, Korea, ^rUniversity of Manchester, Manchester M13 9PL, United Kingdom, ^sQueen Mary, University of London, London, E1 4NS, United Kingdom, ^tUniversity of Melbourne, Victoria 3010, Australia, ^uMuons, Inc., Batavia, IL 60510, USA, ^vNagasaki Institute of Applied Science, Nagasaki, Japan, ^wNational Research Nuclear University, Moscow, Russia, ^xNorthwestern University, Evanston, IL 60208, USA, ^yUniversity of Notre Dame, Notre Dame, IN 46556, USA, ^zUniversidad de Oviedo, E-33007 Oviedo, Spain,

The associated production of the W boson with a single charm quark in proton-antiproton collisions is described at lowest order in the standard model (SM) by quark-gluon fusion ($gq \rightarrow Wc$), where q denotes a d , s , or b quark. At the Tevatron proton-antiproton collider, the larger d quark parton distribution function (PDF) in the proton is compensated by the small quark-mixing (Cabibbo-Kobayashi-Maskawa or CKM) matrix element $|V_{cd}|$, so that only about 20% of the total Wc production rate is due to $gd \rightarrow Wc$, with the majority due to strange quark-gluon fusion. The contribution from $gb \rightarrow Wc$ is also heavily suppressed by $|V_{cb}|$ and the b quark PDF. The Wc production cross section is therefore particularly sensitive to the gluon and s quark PDFs [1, 2], at a momentum transfer Q^2 of the order of the W boson mass (M_W), and to the magnitude of the CKM matrix element

^{aa}CNRS-IN2P3, Paris, F-75205 France, ^{bb}Texas Tech University, Lubbock, TX 79609, USA, ^{cc}Universidad Tecnica Federico Santa Maria, 110v Valparaiso, Chile, ^{dd}Yarmouk University, Irbid 211-63, Jordan,

V_{cs} . Measurements of Wc production in high energy $p\bar{p}$ collisions are of interest because they constrain the proton's s quark PDF at momentum transfers about three orders of magnitude higher than in neutrino-nucleon scattering [3]. Finally, the Wc final state is similar to final state of other processes, such as single top-quark production, neutral and charged Higgs boson production, and supersymmetric top-quark production. The techniques developed here could lead to a better understanding of those samples and their searches. Calculations of $W +$ heavy quark production are available at leading order (LO) and next-to-leading order (NLO) in quantum chromodynamics (QCD) [4], with the NLO cross section prediction about 50% larger than the LO calculation. Overall, the uncertainty on the NLO theoretical expectation for the Wc production cross section at the Tevatron is 10–20%, depending on the charm phase space considered, dominated by uncertainties from the choice of factorization and renormalization scales and the shape of the s quark PDF.

We present the first observation of $p\bar{p} \rightarrow Wc$ production. The charm quark is identified through the semileptonic decay of the charm hadron into an electron or muon (referred to in this Letter as “soft leptons”). This measurement supersedes our previous result [5], where the cross section for $p\bar{p} \rightarrow Wc$ was determined with a precision of approximately 30% and a statistical significance of about 3 standard deviations. The present analysis is performed using a data set more than twice as large and signal events with soft electrons are included to increase the acceptance. The analysis exploits the correlation between the charge of the W boson and the charge of the soft lepton from the semileptonic decay of the charm hadron. Charge conservation in the process $q\bar{q} \rightarrow Wc$ ($q = d, s$) allows only $W^+\bar{c}$ and W^-c final states; as a result the charge of the lepton from the semileptonic decay of the c quark and the charge of the W boson are always of opposite sign, neglecting any effects due to slow-rate charm quark oscillations.

The W boson is identified through its leptonic decay by looking for an isolated electron (muon) carrying large transverse energy E_T (momentum p_T), with respect to the beam line. The neutrino escapes the detector, causing an imbalance of total transverse energy, referred to as “missing E_T ” (\cancel{E}_T) [6]. Quarks hadronize and are observed as jets of charged and neutral particles. Charm jets are identified by requiring an electron or muon candidate within the jet (“soft lepton tagging” or “SLT $_\ell$ ”). Events are classified based on whether the charge of the lepton from the W boson and the charge of the soft lepton are of opposite sign (OS) or same sign (SS). The Wc production cross section is then calculated using the formula

$$\sigma_{Wc} = \frac{N_{\text{tot}}^{OS-SS} - N_{\text{bkg}}^{OS-SS}}{S A \int L dt}, \quad (1)$$

where N_{tot}^{OS-SS} (N_{bkg}^{OS-SS}) is the difference in the number of OS and SS events in data (background), A is the product of the efficiency, for identifying Wc events, with the kinematical and geometrical acceptance, and $\int L dt$ is the integrated luminosity of the data sample. The quantity $S = (N_{Wc}^{OS} - N_{Wc}^{SS}) / (N_{Wc}^{OS} + N_{Wc}^{SS})$ accounts for the charge asymmetry of the sample of real reconstructed Wc events, which is less than unity due to dilution arising from hadronic decays in flight and hadrons misidentified as soft leptons. The terms A and S , which are derived from a Monte Carlo (MC) simulation of Wc events and the detector response, specify the unfolding from the observed same-sign subtracted Wc event yield to the measured cross section. The cross section is defined through A to correspond to the production of a W boson over the entire kinematic range associated with a single charm quark with $p_{Tc} > 20$ GeV/ c , $|\eta_c| < 1.5$. The phase space of the charm is restricted to approximately match the detector acceptance of the charm quark, which minimizes the theoretical uncertainties on A . In the determination of A , the Wc signal is defined to include events with a single charm quark and allows for additional jets; contributions from all sources of W bosons associated with $c\bar{c}$ pairs are not considered in the acceptance since they cancel out in the same-sign subtraction, owing to the largely charge-symmetric detector response.

The CDF II detector is described in detail elsewhere [7]. The data sample, produced in $p\bar{p}$ collisions at $\sqrt{s} = 1.96$ TeV during Run II of the Fermilab Tevatron, was collected between March 2002 and March 2009. This analysis is based on an integrated luminosity of 4.3 ± 0.3 fb $^{-1}$. Events are selected with an inclusive-lepton online event selection (trigger) requiring an electron (muon) with $E_T > 18$ GeV ($p_T > 18$ GeV/ c). The trigger and lepton identification efficiencies are measured using Z boson decays to electrons and muons, and vary between 80% and 97% [8]. Further selection requires exactly one isolated electron (muon), both with isolation parameter $I < 0.1$ [9], with E_T (p_T) greater than 20 GeV (20 GeV/ c) and $|\eta| < 1.1$. The event must also have $\cancel{E}_T > 25$ GeV and exactly one jet with $E_T > 20$ GeV and $|\eta| < 2.0$. The transverse mass of the W boson candidates is required to be greater than 20 GeV/ c^2 [10]. Jets are identified using a fixed-cone algorithm with a cone opening of $\Delta R \equiv \sqrt{(\Delta\eta)^2 + (\Delta\phi)^2} = 0.4$ and are constrained to originate from the $p\bar{p}$ collision vertex. The jet energies are corrected for detector response, multiple interactions, and uninstrumented regions of the detector [11].

Muon candidates inside jets are identified by matching the trajectories of charged particles (tracks) of the jet, as measured in the inner tracking system, with track segments in the muon detectors. An SLT $_\mu$ [8, 12] must have $p_T > 3$ GeV/ c and be within $\Delta R < 0.6$ of a jet axis. Soft electrons from semileptonic heavy-flavor decay (SLT $_e$) are identified by tracks with $p_T > 2$ GeV/ c

that are associated with an electromagnetic shower in the central electromagnetic calorimeter, and must lie within $\Delta R < 0.4$ of a jet axis. Furthermore, finely segmented wire and strip chambers are used to identify the collimated shower of the electron within the broader hadronic shower of the jet. Additional variables to discriminate soft electrons are based on the energy deposition, transverse shower shape, and track-shower distance [13, 14]. To reduce background from $\Upsilon/\gamma^* \rightarrow \mu\mu$ and $Z/\gamma^* \rightarrow \mu\mu$, events are discarded where the invariant mass computed from the oppositely charged soft muon and primary muon is in the 8–11 GeV/ c^2 or 70–110 GeV/ c^2 ranges. Events are also discarded if the jet tagged by a soft muon has an electromagnetic fraction greater than 90%, to reduce the contamination from $Z \rightarrow \mu\mu$ decays with final-state radiation off one muon. For the sample with a soft electron and a candidate $W \rightarrow e\nu$ decay, the events for which the invariant mass between the two electrons is greater than 45 GeV/ c^2 are rejected in order to reduce the background from $Z/\gamma^* \rightarrow ee$ events. To suppress QCD multijet background, we reject events for which the azimuthal angular difference between the \cancel{E}_T and the jet is less than 0.3 rad. In the SLT_μ (SLT_e) channel we find a total of 1482 (2494) OS events and 1024 (2088) SS events that satisfy the above selection criteria, corresponding to a same-sign subtracted excess of 458 (406) events, respectively.

The dominant backgrounds to Wc are due to the associated production of jets with the W boson ($W +$ jets, excluding the Wc under investigation), and from Drell-Yan production of Z/γ^* , with and without additional jets. Multijet QCD events and small contributions from diboson, single top, and $t\bar{t}$ production are also present. Backgrounds are estimated using a combination of MC simulation and control regions from the data. The MC simulations of $W +$ jets and $Z/\gamma^* +$ jets processes are performed using ALPGEN (v2.1 [15]) interfaced with PYTHIA (v6.3 [16]) for the parton shower (PS) evolution. The simulation of the Wc signal is performed similarly and is referred to as LO + PS. Modeling of heavy-quark hadron decay is provided by EVTGEN [17]. All samples are simulated using the CTEQ5L PDF sets, with Tune BW [18] to model the underlying event and the hadronization parameters. Events with a $Z \rightarrow \tau\tau$ decay are also simulated, as well as $Zb\bar{b}$ and $Zc\bar{c}$ final states. The production of $Z/\gamma^* +$ jets in the simulation is normalized by the measured exclusive $Z + 1$ jet cross section [19].

The W boson events that can mimic the Wc signature consist of a W boson associated with heavy-flavor quark pairs ($b\bar{b}$ and $c\bar{c}$) or light-flavor (LF) jets. However, since this measurement is sensitive to the excess of OS over SS events, backgrounds that lead to an equal amount of SS and OS events will not contribute to the OS excess ascribed to Wc . Therefore, while the reconstructed $Wb\bar{b}$ and $Wc\bar{c}$ events that pass the selection requirements are approximately as many as those from the

Wc signal, they are nearly completely charge symmetric, since the soft lepton can come from either the b (c) or \bar{b} (\bar{c}), and the excess of OS over SS events from $Wb\bar{b}$ and $Wc\bar{c}$ is negligible. On the other hand, $W +$ LF events enter the data sample when the jet is identified as a charm jet via a misreconstructed soft electron or soft muon tag (“mistagging”). Since the same process that leads to Wc production describes Wu , a small anti-correlation between the charge of the W boson and the charge-sign of the tracks in the jets recoiling against the W is also observed, leading to a residual background contribution. We rely on a combination of MC simulations and data-driven techniques to estimate this contribution to the tagged sample: First the number of $W +$ jets events ($\simeq 97\%$ of which is $W +$ LF) is estimated in the sample of events before tagging the jet (“pretag sample”) by subtracting from the data the initial pretag estimate of the signal and all other backgrounds. The number of tagged $W +$ jets events is obtained from this pretag estimate using a mistag probability parametrization. The procedures for measuring the contribution from real and misidentified lepton tags for both the SLT_μ and SLT_e were developed in previous data analyses [8, 13]; calibrations were derived using independent samples, validated in $b\bar{b}$ events, and used for the $t\bar{t}$ cross section measurements. The probability of misidentifying a hadron as an SLT_μ , denoted as the SLT_μ mistag probability, is measured using a data sample of pions, kaons, and protons from Λ^0 and D^{*+} -tagged D^0 decays. It is parametrized as a function of the track curvature and η , and is shown to describe within $\pm 5\%$ the number of false SLT_μ tags in candidate light-flavor jets of QCD multijet and $\gamma +$ jet events. A fraction (0.34 ± 0.02)% of the $W +$ LF pretag events is expected to be mistagged with a soft muon. The SLT_e mistag probability is estimated using MC simulation and checked on a data sample of light-flavor jets from QCD multijet events, and a fraction (0.89 ± 0.07)% of the $W +$ LF pretag events is expected to be mistagged with a soft electron. Both these uncertainties include the systematic uncertainty from the corresponding mistag probability parametrization. The SLT_e mistag probability is higher than that of SLT_μ also due to contributions from photon conversions. The charge asymmetry in $W +$ LF is determined directly from the data by applying the mistag parametrizations to tracks in the $W +$ jet pretagged sample; for the SLT_e , the asymmetry is then corrected for the 20% contribution to $W +$ LF tags from conversions, which is charge symmetric and does not affect the charge correlation of tracks in the pretagged sample. The result is in agreement with estimates using a simulation of $W +$ LF jets.

The second largest background to Wc is due to the misreconstruction of $Z/\gamma^* +$ jets events. The two leptons from the Z/γ^* decay can be misidentified as one lepton from a W boson decay and one soft lepton, resulting in approximately 90% charge asymmetry. These

events are suppressed by the veto on the Z -mass region. Alternatively, only one lepton from the Z boson decay is reconstructed in the event, which is typically assigned to be a W -decay lepton. In this case, the soft lepton results from the decay of heavy flavor or from the misreconstruction of a track from hadrons, and these events carry approximately 40% asymmetry. The overall average charge asymmetry of $Z/\gamma^* + \text{jets}$ for SLT_e is smaller than for SLT_μ because of the stricter requirements on the dielectron mass.

Events due to QCD multijet production can enter the selection through hadronic misidentification or heavy-flavor decay. Missing transverse energy can arise from mismeasured jet energy, detector effects, or neutrinos in the decay chain. We estimate this background by releasing the missing energy requirement on the events and fitting templates of the \cancel{E}_T distribution for the QCD multijet component, separately for OS and SS events. The template distribution for QCD multijet events is derived from a jet-enriched data sample in which candidate electrons fail two of the electron identification criteria. The remaining sample composition is modeled with MC simulations.

Finally, the production of dibosons (WW, WZ, ZZ) and $t\bar{t}$ is modeled with a PYTHIA (v6.4) MC calculation, while single top-quark production is simulated using MADEVENT [20]. These processes together contribute a few percent of the total background, and their production cross sections are well established. The WW events contribute the most and have a strong charge asymmetry. Table I summarizes the data and the estimated background.

We assume that the total OS–SS rates observed in the data, after subtracting the background contributions listed in Table I, are due to the Wc signal; the SS-subtracted rates for the signal are then $287 \pm 50(\text{stat}) \pm 32(\text{syst})$ and $149 \pm 68(\text{stat}) \pm 26(\text{syst})$ events, for the SLT_μ and SLT_e tagged samples, respectively. This is higher than the number of OS–SS events predicted by the LO + PS simulation of Wc production. Figure 1 shows the distributions of the measured p_T spectrum for SLT muons and electrons in tagged events, compared to the predicted spectrum given by the Wc signal and estimated background. For each contribution, SS events are subtracted. The Wc production cross section is calculated using Eq. (1), with $\sigma_{Wc} \equiv \sigma_{W+\bar{c}} + \sigma_{W-c}$, $B(W \rightarrow \ell\nu) = 0.108 \pm 0.009$ [21], $p_{Tc} > 20 \text{ GeV}/c$, and $|\eta_c| < 1.5$; the values of the dilution S for Wc events are given in Table I. We measure $\sigma_{Wc} \times B(W \rightarrow \ell\nu) = 13.4 \pm 2.3(\text{stat})^{+2.5}_{-2.0}(\text{syst})^{+1.2}_{-1.0}(\text{lum})$ pb and $\sigma_{Wc} \times B(W \rightarrow \ell\nu) = 15.0 \pm 6.8(\text{stat})^{+4.4}_{-2.9}(\text{syst}) \pm 1.2(\text{lum})$ pb from the SLT_μ and SLT_e samples, respectively.

Systematic uncertainties are shown in Table II. The uncertainty on the SLT tagging includes contributions from the measurements of the efficiency of tagging leptons in a jet environment and of mistagging [8, 13]. The

TABLE I: Summary of data and backgrounds in the SLT_μ -tagged and SLT_e -tagged $W + 1$ jet samples. The expected Wc contribution is shown from a LO + PS calculation.

Source	Events	Asymmetry	OS–SS
SLT_μ			
$W + \text{LF}, bb, c\bar{c}$	1808 ± 271	0.05 ± 0.01	86 ± 14
$Z/\gamma^* + \text{jets}$	132 ± 30	0.63 ± 0.02	84 ± 18
QCD multij.	308 ± 17	-0.03 ± 0.07	-8 ± 17
Diboson, $t(\bar{t})$	26 ± 3	0.33 ± 0.01	9 ± 1
Wc (LO + PS)	214 ± 19	0.75 ± 0.03	161 ± 13
Total expected	2488 ± 274	–	331 ± 37
Data	2506	–	458
SLT_e			
$W + \text{LF}, bb, c\bar{c}$	4076 ± 305	0.04 ± 0.01	174 ± 19
$Z/\gamma^* + \text{jets}$	138 ± 29	0.26 ± 0.01	36 ± 7
QCD multij.	374 ± 12	0.07 ± 0.03	27 ± 12
Diboson, $t(\bar{t})$	35 ± 3	0.58 ± 0.01	20 ± 2
Wc (LO + PS)	174 ± 16	0.45 ± 0.02	78 ± 7
Total expected	4797 ± 307	–	336 ± 28
Data	4582	–	406

TABLE II: Summary of systematic uncertainties, as a percentage of the measured Wc cross section. Numbers shown in bold font indicate uncertainties treated as uncorrelated in the combination of the channels.

Source	SLT_μ	SLT_e
SLT uncertainties	± 9.2	± 16.6
QCD multijet estimate	± 6.3	± 9.9
Initial and final state radiation	± 6.0	± 6.0
Background cross sections	± 5.7	± 4.7
c quark hadronization	± 4.6	± 4.6
PDFs	± 3.6	± 3.6
W -lepton ID	± 2.2	± 2.2
Jet energy calibration	± 2.0	± 2.0
Factorization, renormalization scales	± 1.3	± 1.3
Total	± 15.4	± 21.8
Luminosity	± 7.9	± 8.3

uncertainty on the backgrounds includes contributions from the theoretical cross sections, from the estimation technique, and from statistics for the backgrounds evaluated with inputs from a data control region. For the Z/γ^* background, the dominant uncertainty on the event yield estimate comes from the measured Z cross section uncertainty. To measure the effects of initial- and final-state gluon radiation, we measure the Wc acceptance in different samples with the radiation enhanced or reduced, as in Ref. [22]. We compare charm jets modelled with the

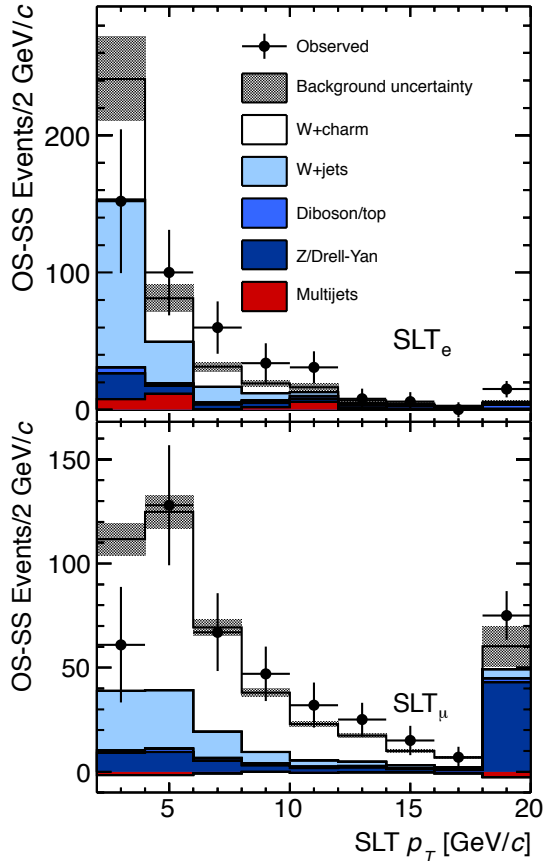


FIG. 1: The soft muon and soft electron p_T distributions. The Wc contribution is derived from a LO + PS simulation normalized to the measured cross section.

PYTHIA and HERWIG [23, 24] MC calculations to evaluate the uncertainty due to different hadronization models. The PDF uncertainty is derived by remeasuring the acceptance using the CTEQ and MRST sets, following the same prescription as in Ref. [22]. The MC modeling of the efficiency for identifying the leptons from the W boson decay (“ W lepton ID”) is measured using Z boson data and MC samples. The charge misidentification rate is less than 1% and therefore has a negligible effect. The uncertainty due to the jet energy calibration (JES) is measured by shifting the energies of the jets in the Wc MC simulation by $\pm 1\sigma$ of the JES [11]. The uncertainty on the acceptance due to the factorization and renormalization scales is estimated by varying them in the ALPGEN MC between 1/2 and twice the transverse mass of the W boson, as well as using the charm quark p_T .

The results from the two SLT-tagged samples are combined by performing a profile likelihood ratio minimization [25]. Systematic uncertainties are in-

cluded as nuisance parameters with Gaussian constraints whose widths are fixed to the respective uncertainties, and are assumed to be either fully correlated, if they are shared between the two channels, or uncorrelated if not. The combination of the cross section yields $\sigma_{Wc}(p_{Tc} > 20 \text{ GeV}/c, |\eta_c| < 1.5) \times B(W \rightarrow \ell\nu) = 13.6 \pm 2.2(\text{stat})_{-1.9}^{+2.3}(\text{syst}) \pm 1.1(\text{lum}) \text{ pb} = 13.6_{-3.1}^{+3.4} \text{ pb}$. The significance for the Wc signal is derived from the ratio of profile-likelihoods λ , with $-2\ln\lambda$ in the hypothesis of no signal being interpreted as following a χ^2 -distribution, and is calculated to be 5.7σ . The measurement is in agreement with a NLO calculation over the same phase space of $11.4 \pm 1.3 \text{ pb}$ [26], where the renormalization and factorization scales have been set to half the W boson mass, and varied between 5 GeV and 80 GeV in the uncertainty. The uncertainty also includes PDF variations using the CTEQ6M and MSTW2008 sets. The result can be also compared to the LO prediction of $8.2 \pm 1.5 \text{ pb}$ [26], giving a measurement to LO cross section ratio for this kinematic region of 1.6 ± 0.5 . Since the majority of Wc production proceeds through c to s quark coupling, we can relate the measured value of the cross section with the theoretical prediction and derive $|V_{cs}|$. Using $\sigma_{Wc}^{\text{theory}} = 9.8(\pm 1.1)|V_{cs}|^2 + 2.1(\pm 0.2) \text{ pb}$ [26] we obtain $|V_{cs}| = 1.08 \pm 0.16$, where the uncertainties in the cross section measurement and in the theoretical prediction have been added in quadrature. Restricting the range of $|V_{cs}|$ to the interval $[0,1]$, a lower limit of $|V_{cs}| > 0.71$ at the 95% confidence level is extracted.

In conclusion, we present the first observation of production of a W boson associated to a single charm quark, with a significance of 5.7 standard deviations. This is obtained in data corresponding to 4.3 fb^{-1} produced in $p\bar{p}$ collisions at $\sqrt{s} = 1.96 \text{ TeV}$ and collected by the CDF experiment. The measured cross section is $\sigma_{Wc}(p_{Tc} > 20 \text{ GeV}/c, |\eta_c| < 1.5) \times B(W \rightarrow \ell\nu) = 13.6_{-3.1}^{+3.4} \text{ pb}$, which is in agreement with a SM NLO calculation. A direct determination of $|V_{cs}| = 1.08 \pm 0.16$ and the 95% C.L. lower limit of $V_{cs} > 0.71$ are extracted assuming that the Wc production through c to s quark coupling is dominant.

We thank the Fermilab staff and the technical staffs of the participating institutions for their vital contributions. This work was supported by the U.S. Department of Energy and National Science Foundation; the Italian Istituto Nazionale di Fisica Nucleare; the Ministry of Education, Culture, Sports, Science and Technology of Japan; the Natural Sciences and Engineering Research Council of Canada; the National Science Council of the Republic of China; the Swiss National Science Foundation; the A.P. Sloan Foundation; the Bundesministerium für Bildung und Forschung, Germany; the Korean World Class University Program, the National Research Foundation of Korea; the Science and Technology Facilities Council, the Royal Society and the Leverhulme Trust, UK; the Russian Foundation for Basic Research; the Ministero de

Ciencia e Innovación, and Programa Consolider-Ingenio 2010, Spain; the Slovak R&D Agency; the Academy of Finland; and the Australian Research Council (ARC).

-
- [1] U. Baur, F. Halzen, S. Keller, M.L. Mangano, and K. Riesselmann, *Phys. Lett. B* **318**, 544 (1993).
- [2] H.L. Lai, P. Nadolsky, J. Pumplin, D. Stump, W. Tung, and C. Yuan, *J. High Energy Phys.* 4 (2007) 089.
- [3] M. Goncharov *et al.* (NuTeV Collaboration), *Phys. Rev. D* **64**, 112006 (2001).
- [4] S. Keller, W.T. Giele, and E. Laenen, *Phys. Lett. B* **372**, 141 (1996).
- [5] A. Abulencia *et al.* (CDF Collaboration), *Phys. Rev. Lett.* **100**, 091803 (2008).
- [6] We use a (z, ϕ, θ) coordinate system where the z -axis is in the direction of the proton beam, and ϕ and θ are the azimuthal and polar angles, respectively. The pseudorapidity is $\eta \equiv -\ln(\tan \frac{\theta}{2})$. Transverse energy and momentum are $E_T \equiv E \sin \theta$ and $p_T \equiv p \sin \theta$, respectively, where E and p are energy and momentum. The missing transverse energy is $\cancel{E}_T \equiv |-\sum_i E_T^i \hat{n}_i|$, where E_T^i is the magnitude of the transverse energy contained in each calorimeter tower i in the region $|\eta| < 3.6$, and \hat{n}_i is the direction unit vector of the tower in the plane transverse to the beam direction.
- [7] The CDF II Detector Technical Design Report, Fermilab-Pub-96/390-E; D. Acosta *et al.* (CDF Collaboration), *Phys. Rev. D* **71**, 052003 (2005).
- [8] D. Acosta *et al.* (CDF Collaboration), *Phys. Rev. D* **79**, 052007 (2009).
- [9] The isolation (I) is defined as the calorimeter transverse energy in a cone of opening $\Delta R \equiv \sqrt{(\Delta\eta)^2 + (\Delta\phi)^2} = 0.4$ around the lepton (not including the lepton energy itself) divided by the lepton E_T or p_T .
- [10] The transverse mass of the W boson ($M_{T,W}$) is defined as $M_{T,W} = \sqrt{2p_{T,\ell}\cancel{E}_T(1 - \cos\Delta\phi_{\ell,\nu})}$, where $p_{T,\ell}$ is the lepton transverse momentum, \cancel{E}_T is the missing transverse energy in the event, and $\Delta\phi_{\ell,\nu}$ is the angle in the $r - \phi$ plane between the two.
- [11] A. Bhatti *et al.*, *Nucl. Instrum. Methods Phys. Res., Sect A* **566**, 2 (2006).
- [12] D. Acosta *et al.* (CDF Collaboration), *Phys. Rev. D* **72**, 032002 (2005).
- [13] D. Acosta *et al.* (CDF Collaboration), *Phys. Rev. D* **81**, 092002 (2010).
- [14] J. P. Chou, Ph.D. thesis, Harvard University, FERMILAB-THESIS-2008-93 (2008).
- [15] M. L. Mangano, F. Piccinini, A.D. Polosa, M. Moretti, and R. Pittau, *J. High Energy Phys.* 07 (2003) 001.
- [16] T. Sjostrand, P. Eden, C. Friberg, L. Lonnblad, G. Miu, S. Mrenna, and E. Norrbin, *Comput. Phys. Commun.* **135**, 238 (2001).
- [17] D. Lange, *Nucl. Instrum. Methods Phys. Res., Sect A* **462**, 1 (2001).
- [18] H.L. Lai, J. Huston, S. Kuhlmann, J. Morfin, F. Olness, J.F. Owens, J. Pumplin, and W.K. Tung, *Eur. Phys. J. C* **12**, 375 (2000).
- [19] D. Acosta *et al.* (CDF Collaboration), *Phys. Rev. Lett.* **94**, 091803 (2005); *Phys. Rev. Lett.* **100**, 102001 (2008).
- [20] F. Maltoni and T. Stelzer, *J. High Energy Phys.* 2 (2003) 027.
- [21] J. Beringer *et al.* (Particle Data Group), *Phys. Rev. D* **86**, 010001 (2012).
- [22] A. Abulencia *et al.* (CDF Collaboration), *Phys. Rev. D* **73**, 032003 (2006).
- [23] G. Marchesini and B.R. Webber, *Nucl. Phys.* **B310**, 461 (1988).
- [24] G. Corcella, I.G. Knowles, G. Marchesini, S. Moretti, K. Odagiri, P. Richardson, M.H. Seymour, and B.R. Webber, *J. High Energy Phys.* 01 (2001) 010.
- [25] G. Cowan, K. Cranmer, E. Gross and O. Vitells, *Eur. Phys. J. C* **71**, 1554 (2011).
- [26] J.M. Campbell and R.K. Ellis, *Phys. Rev. D* **60**, 113006 (1999).